

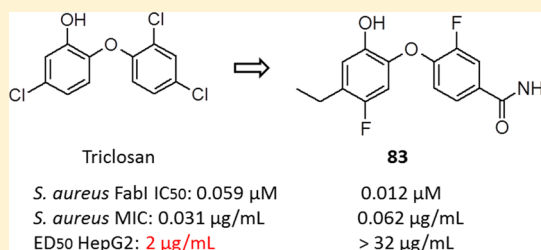
## From Triclosan toward the Clinic: Discovery of Nonbiocidal, Potent FabI Inhibitors for the Treatment of Resistant Bacteria

Vincent Gerusz,<sup>\*,†</sup> Alexis Denis,<sup>†,§</sup> Fabien Faivre,<sup>†</sup> Yannick Bonvin,<sup>†</sup> Mayalen Oxoby,<sup>†</sup> Sophia Briet,<sup>†</sup> Géraldine LeFralliec,<sup>†</sup> Chrystelle Oliveira,<sup>†</sup> Nicolas Desroy,<sup>†,||</sup> Cédric Raymond,<sup>†</sup> Laëticia Peltier,<sup>†,||</sup> François Moreau,<sup>‡</sup> Sonia Escaich,<sup>‡,⊥</sup> Vanida Vongsouthi,<sup>‡</sup> Stéphanie Floquet,<sup>‡</sup> Elodie Drocourt,<sup>‡</sup> Armelle Walton,<sup>‡</sup> Laure Prouvensier,<sup>‡</sup> Marc Saccomani,<sup>‡</sup> Lionel Durant,<sup>‡,#</sup> Jean-Marie Genevard,<sup>‡</sup> Vanessa Sam-Sambo,<sup>‡</sup> and Coralie Soulama-Mouze<sup>‡,∞</sup>

<sup>†</sup>Medicinal Chemistry and <sup>‡</sup>Biology, Mutabilis, 102 Avenue Gaston Roussel, 93230 Romainville, France

### Supporting Information

**ABSTRACT:** In this paper, we present some elements of our optimization program to decouple triclosan's specific FabI effect from its nonspecific cytotoxic component. The implementation of this strategy delivered highly specific, potent, and nonbiocidal new FabI inhibitors. We also disclose some preclinical data of one of their representatives, **83**, a novel antibacterial compound active against resistant staphylococci and some clinically relevant Gram negative bacteria that is currently undergoing clinical trials.



### INTRODUCTION

The increase of antimicrobial resistance has become a global healthcare problem, rendering obsolete many antibiotic therapies.<sup>1,2</sup> Among Gram-positive pathogens, the emergence and spread of multidrug resistant *Staphylococcus aureus* constitute a well-known problem.<sup>3–5</sup> There is therefore an urgent medical need for new antibacterial drugs, especially with novel mechanisms of action that would display minimal cross-resistance with currently used treatments.

The bacterial fatty acid biosynthesis pathway has generated much interest for the development of such novel class agents.<sup>6,7</sup> The organization of the bacterial fatty acid synthase type II system based on individual enzymes (FASII system, Figure 1) is different from the multifunctional fatty acid synthase type I system found in eukaryotes, therefore providing good prospects for selective inhibition. Moreover, all the representative targets of the FASII system have already been characterized by X-ray crystallography or NMR, which should facilitate the rational design of inhibitors. Although recent communications have expressed some concern about the validity of FASII as antibiotic targets for Gram-positive pathogens,<sup>8,9</sup> counterexperiments have brought some evidence to the essentiality of this pathway for *S. aureus*.<sup>10–12</sup> While human clinical efficacy data would be needed to close this debate, significant work continues by both academic groups and the pharmaceutical industry to validate the FASII targets and discover relevant inhibitors.<sup>13</sup>

The last step of the fatty acid elongation cycle is catalyzed by enoyl-ACP reductases. Among them, FabI constitutes the single isoform in major pathogens such as *S. aureus*,<sup>14</sup> *Escherichia coli*,<sup>15</sup> and *Mycobacterium tuberculosis*<sup>16</sup> (also called InhA for the last). The clinical success of the InhA inhibitor isoniazid<sup>17</sup> and

numerous reports of FabI inhibitors<sup>18</sup> involving diazaborines,<sup>19</sup> 4-pyridones,<sup>20</sup> naphthyridinones,<sup>21</sup> triclosan,<sup>22</sup> and analogues<sup>23–30</sup> have validated this target as one of the most attractive of the FASII pathway. Although a couple of these inhibitors have entered clinical trials,<sup>31,32</sup> none of them have made it yet to market.

Triclosan is a widely used broad-spectrum biocide,<sup>33</sup> which also displays reversible inhibition of *E. coli* FabI.<sup>34</sup> Despite its biocidal component and intravenous toxicity warranting against a systemic use,<sup>35</sup> it can still be considered as an attractive lead for a number of reasons. Indeed, its active site entry results in a reordering of a loop of amino acids, making it a slow, tight-binding inhibitor<sup>36</sup> with a long residence time that has been correlated with in vivo activity.<sup>37</sup> Its picomolar  $K_i$  for binding the enzyme–cofactor complex<sup>34</sup> and low molecular weight also entail a high ligand efficiency,<sup>38</sup> and finally there is a variety of available costructures.<sup>34,36,39,40</sup>

In this report, we describe our drug design efforts to harvest its potency without its biocidal component. We also disclose some elements of structure–activity relationships (SARs) that led to the identification of a potent antistaphylococcal clinical candidate.

### CHEMISTRY

The synthetic routes used to prepare the left-part derivatives of Table 1 are illustrated in Scheme 1. Guaiaicol **1** was substituted by pyridine **2** under basic conditions to provide the phenoxy pyridine **3**, which was demethylated with boron tribromide to afford the final compound **4**. This general

Received: July 30, 2012

Published: October 23, 2012

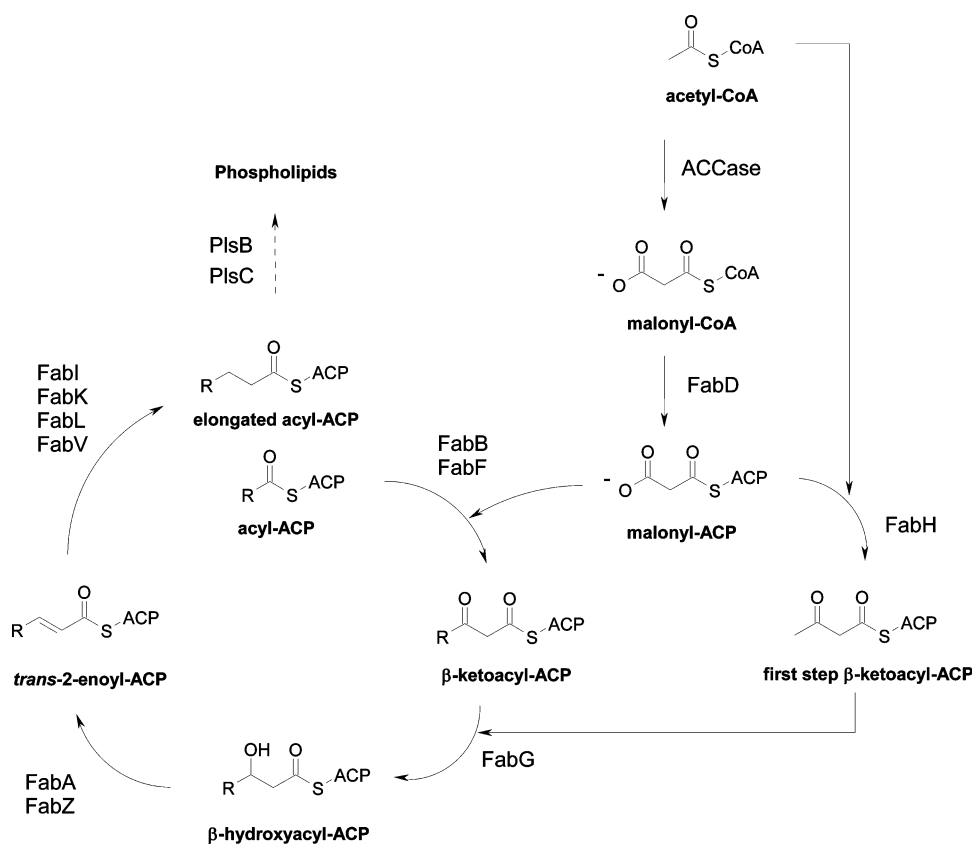


**Figure 1.** Schematic representation of FASII system.

procedure was used to provide the other analogues, with in some instances additional steps to prepare specific side chains. The left-part moiety of **56** was obtained by Negishi cross-coupling reaction of halide **5** with isobutylzinc bromide. Reaction of **7** with Ruppert–Prakash reagent and tetrabutylammonium fluoride provided the common hydroxyl intermediate **8**, which was either dehydroxylated via tosylation and hydrogenation to afford the trifluoroethyl side chain of **57** or fluorinated using diethylaminosulfur trifluoride and dehydrofluorinated under basic conditions to yield the trifluorovinyl side chain of **58**. Compound **11** was submitted to Suzuki coupling with 4-methylphenylboronic acid to provide intermediate **12** bearing the left-part of **59**. Compound **13** was chlorinated using mesyl chloride to afford **14**, which was in turn demethylated with boron tribromide and methoxylated by displacement of the chloride with sodium methoxide to provide **15**. Alternatively, the chloro intermediate **14** was substituted with imidazole under sodium hydride conditions to yield the side chain of **62** and in similar fashion compounds **63** and **64**.

A variety of methods were utilized to prepare the right-part derivatives of Table 2 as illustrated in Scheme 2. Guaiacol **1** was coupled to 4-methoxyphenylboronic acid under copper acetate conditions to provide **17**, which was monodemethylated using boron tribromide to provide **65**. Compounds **66**, **67**, and **68** were obtained in a similar fashion. The side chain of **69** was elaborated by deprotonating intermediate **18** with *s*-butyllithium followed by substitution with 2-bromomethyl-1,3-dioxolane. Compound **70** was obtained by reacting catechol **20** with 2-fluoronitrobenzene under basic conditions followed by reduction under hydrogenation conditions and the usual demethylation using boron tribromide. Intermediate **23** and compounds **71** and **73** were prepared similarly, while

compound **72** was derived from methylation of aniline **21** using formylation with freshly prepared acetic formic anhydride followed by borane reduction. Chlorosulfonylation via the diazonium of **23** followed by reaction with ammonia afforded **24**, which was demethylated to provide **74** and in a similar fashion compounds **75**, **76**, and **77**. Reductive amination of common intermediate **23** yielded **25** bearing the side chain of **78**, while its sulfonylation using cyclopropanesulfonyl chloride afforded **26** to provide **79**. Tosylation of catechol **20** followed by demethylation using boron tribromide led to **27**. Benzylation followed by removal of the tosyl group under magnesium conditions provided **28**, which was reacted with 3,4-difluoronitrobenzene under basic conditions and reduced using tin chloride to afford **29**. Substitution of this aniline with 3-bromo-1-propanol under basic conditions and subsequent debenylation using palladium hydroxide and ammonium formate delivered compound **30**. Reacting intermediate **29** with benzyl chloroformate followed by deprotonation with *n*-butyllithium and cyclization with racemic glycidyl butyrate provided oxazolidinone **31**. Mesylation of this intermediate, displacement of the mesyl group with sodium azide, and reduction of the benzyl and azide groups under hydrogenation conditions followed by N-acetylation afforded oxazolidinone **32**. Compound **33** was obtained by reacting **20** with 3',4'-difluoroacetophenone under basic conditions followed by demethylation, while further addition of *O*-methylhydroxylamine provided the oxime **34**.

The synthetic routes leading to the derivatives of Table 3 are described in Scheme 3. The acylation of catechol **35** with acetyl chloride and aluminum trichloride provided **36**, which upon reduction using zinc and reaction with 1,2-difluorophenyl afforded **38**. Demethylation under standard conditions using

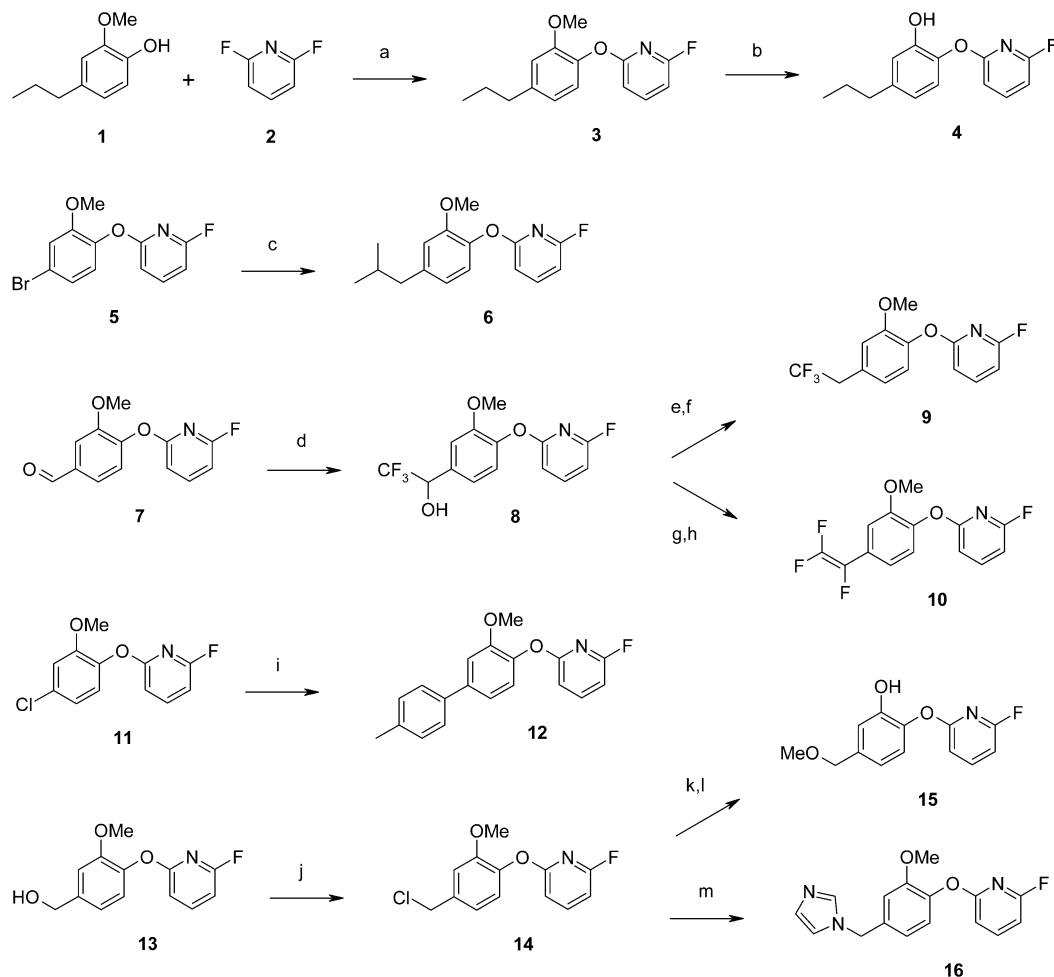
Table 1. FabI Inhibition and Antibacterial Activity of Left-Part Derivatives

Compound	Structure	IC <sub>50</sub> (μM)		MIC (μg/mL)		
		<i>E. coli</i> FabI	SAU <sup>a</sup>	ECO <sup>b</sup>	EFA <sup>c</sup>	SPN <sup>d</sup>
Triclosan		0.170	0.031	0.125	2	8
52		0.550	0.25	0.25	>32	64
53		0.120	0.25	1	>32	64
54		3.5	4	16	>32	>32
55		0.590	0.25	4	>32	>64
4		0.970	0.25	4	>32	64
56		0.570	1	4	>32	>32
57		0.470	0.25	4	>32	>64
58		0.850	1	16	>32	>32
59		6.5	8	8	>32	16
60		29	4	>32	>32	>32
15		14	4	16	>32	>32
61		3.4	1	16	>32	>32
62		56	16	>32	>32	>32
63		5.2	4	16	>32	>32
64		6.9	4	>32	>32	>32

<sup>a</sup>SAU: *S. aureus* CIP54,146 (CRBIP Pasteur Institute). <sup>b</sup>ECO: *E. coli* C7 (O18:K1:H7, Robert Debré Hospital). <sup>c</sup>EFA: *E. faecalis* ATCC29212 (CRBIP Pasteur Institute). <sup>d</sup>SPN: *S. pneumoniae* D39 (Pasteur Institute).

boron tribromide provided compound **81**. Compounds **39**, **41**, and **43** were obtained in a similar way as intermediate **21** of

Scheme 2. Reacting **39** with sodium nitrite and tetrafluoroboric acid provided **40** as the methylated precursor of **80**. Compound

Scheme 1. Synthesis of Table 1 Compounds<sup>a</sup>

<sup>a</sup>Reagents and conditions: (a) KOH, DMF, 110 °C (86%); (b) BBr<sub>3</sub>, DCM, -78 to -20 °C (38%); (c) isobutylzinc bromide, Pd(PPh<sub>3</sub>)<sub>4</sub>, dioxane, 105 °C (20%); (d) (i) trifluoromethyltrimethylsilane, TBAF, THF, rt, (ii) aqueous HCl (88%); (e) TsCl, DMAP, TEA, DCM, 0° to rt (41%); (f) H<sub>2</sub>, Pd/C, rt (80%); (g) DAST, DCM, -78 °C to rt (37%); (h) LiHMDS, THF, 0 °C to rt (43%); (i) 4-methylphenylboronic acid, K<sub>2</sub>CO<sub>3</sub>, Pd(PPh<sub>3</sub>)<sub>4</sub>, DME, water, 105 °C (quant); (j) MsCl, pyridine, DCM, -40 °C to rt (47%); (k) BBr<sub>3</sub>, DCM, -78 to -20 °C (95%); (l) MeONa, NaI, MeOH, rt (quant); (m) imidazole, NaH, DMF, 40 °C (93%).

42 was prepared by treating 41 with boron tribromide followed by sodium borohydride. Hydrolysis of nitrile 43 using trifluoroacetic acid and sulfuric acid provided amide 44, while basic treatment with sodium hydroxide led to carboxylic acid 45, both methylated precursors of compounds 83 and 87. Carboxylic acid 45 was chlorinated with oxalyl chloride and coupled to methylamine to afford upon phenolic demethylation 84 in a procedure also used to provide compounds 85 and 86.

The 3-pyridyl derivatives of Table 4 were prepared according to the synthetic routes illustrated in Scheme 4. Substitution of catechol 47 with 3-fluoro-2-nitropyridine under basic conditions followed by Suzuki coupling of vinylboronic acid pinacol ester and reduction of the vinyl moiety to the ethyl group under hydrogenation conditions provided 49. Demethylation of intermediate 49 using boron tribromide led to compound 94, while a Balz–Schiemann reaction provided 50 and 51, which were demethylated in the usual manner to afford compounds 95 and 96.

The intractable mixture of pyrimidines 89 and 90 was obtained by two different synthetic routes illustrated in Scheme 5. In one pathway, catechol 1 was substituted with 2-chloropyrimidine under basic condition and demethylated

using boron tribromide. In another pathway, tosylation of 1 with tosyl chloride followed by demethylation with boron tribromide, benzylation with benzyl bromide, and tosyl deprotection under basic conditions provided intermediate 92. Substitution with 2-chloropyrimidine under basic conditions and benzyl group hydrogenolysis then converted 92 into the same mixture of 89 and 90.

## RESULTS AND DISCUSSION

FabI is prone to a large degree of induced fit because of a flexible loop encompassing its active site,<sup>36</sup> which may hamper the success of docking studies.<sup>41,42</sup> We therefore decided to engage at first in a SAR-led rational optimization mainly based on enzymatic and antibacterial activity. The decoupling of the nonspecific biocidal action of triclosan was set as one of our major objectives, which was monitored by the absence of antibacterial activity on FabI-independent strains such as *Enterococcus faecalis* (for whom FabI is complemented by FabK) and *Streptococcus pneumoniae* (harboring FabK only).<sup>43</sup>

Triclosan optimization was initiated by investigating the replacement of the 5-chloro group on its catechol by other functionalities. Indeed, superimposing triclosan from an InhA

Table 2. FabI Inhibition and Antibacterial Activity of Aromatic Right-Part Derivatives

Compound	Structure	IC <sub>50</sub> (μM)				MIC (μg/mL)					
		<i>E. coli</i> FabI	SAU <sup>a</sup>	ECO <sup>b</sup>	EFA <sup>c</sup>	SPN <sup>d</sup>	<i>E. coli</i> FabI	SAU <sup>a</sup>	ECO <sup>b</sup>	EFA <sup>c</sup>	SPN <sup>d</sup>
Triclosan		0.170	0.031	0.125	2	8					
65		0.230	0.25	4	>32	>32					
66		3.1	1	16	>32	>32					
67		44	16	>32	>32	>32					
68		0.810	0.25	16	>32	>32					
69		0.380	0.25	16	>32	>32					
70		0.160	0.25	4	>32	>32					
71		42	1	16	>32	16					
72		112	4	>32	>32	>32					
73		0.140	0.25	1	>32	>32					
74		0.860	0.25	1	>32	>32					
75		0.240	0.062	4	>32	16					
76		0.150	0.25	16	>32	>32					
77		1.2	0.25	16	>32	>32					
30		1	0.25	16	>32	>32					
78		0.850	0.25	16	>32	16					
79		2.3	1	16	>32	>32					
33		0.110	0.062	1	16	16					
34		14	1	>32	>32	16					
32		6.1	4	>32	>32	>32					

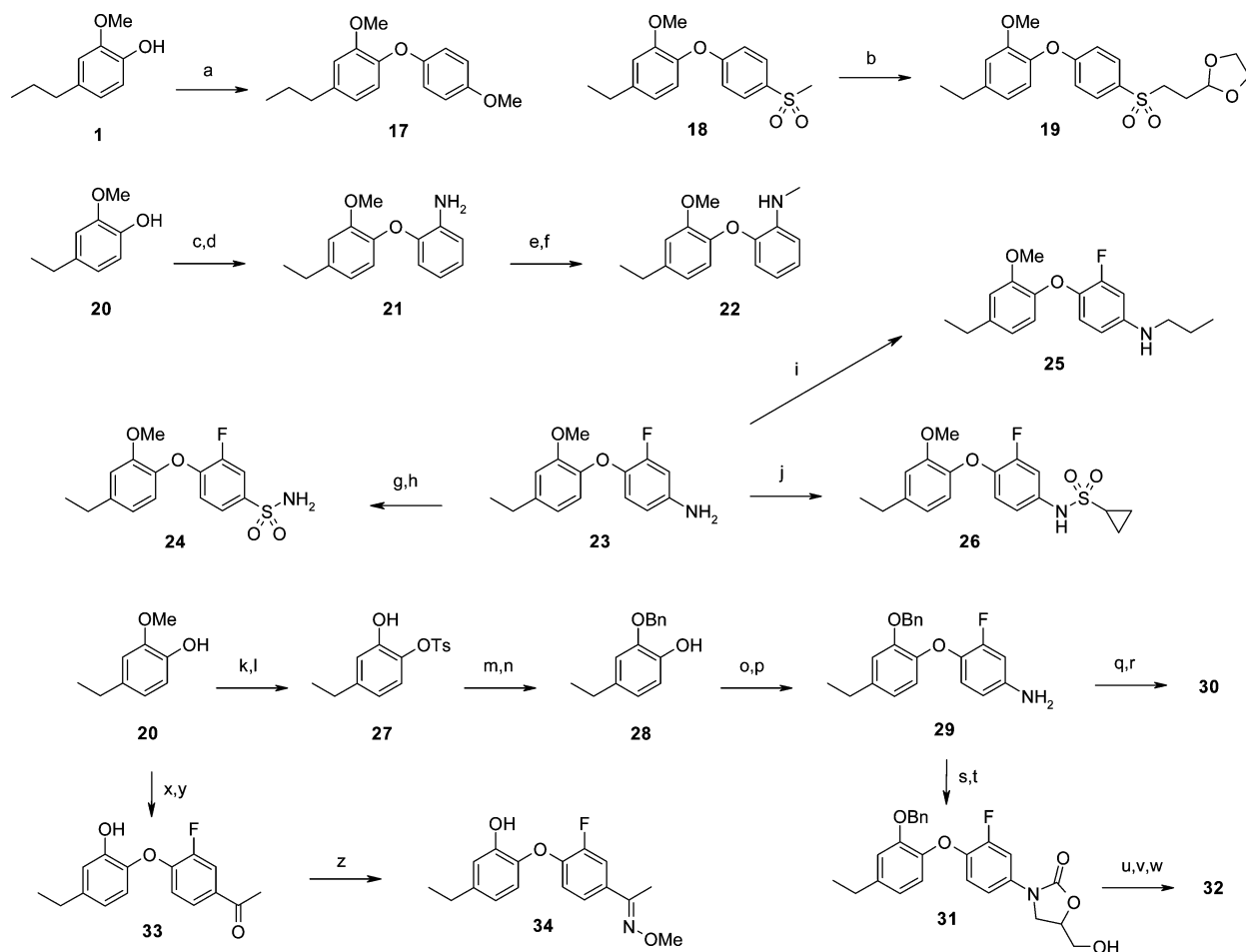
<sup>a</sup>SAU: *S. aureus* CIP54,146 (CRBIP Pasteur Institute). <sup>b</sup>ECO: *E. coli* C7 (O18:K1:H7, Robert Debré Hospital). <sup>c</sup>EFA: *E. faecalis* ATCC29212 (CRBIP Pasteur Institute). <sup>d</sup>SPN: *S. pneumoniae* D39 (Pasteur Institute).

costructure (1P45)<sup>44</sup> to the active site of InhA complexed with NAD<sup>+</sup> and a C16-fatty acid substrate (1BVR)<sup>45</sup> reveals that the 5-chloro group is overlaying well with the alkyl chain of the substrate, with space available in this direction to probe other side chains (Figure 2). Since this area appears lipophilic, most of our new substituents were selected to match this characteristic, although a number of more hydrophilic ones were also evaluated to investigate a potential unexpected induced fit. To facilitate rapid synthetic access to the final products, the novel side chain catechols were coupled to 2,6-difluoropyridine. This right part, although slightly less active than triclosan's dichlorophenyl, was found to maintain enough potency to allow SAR studies on the left-part derivatives and is interestingly almost devoid of nonspecific action (Table 1, compound 52).

Substituting the chloride by a bromide leads to better enzymatic affinity that however does not translate to an increase of antibacterial activity in *E. coli* (53 vs 52). Alkyl and fluoroalkyl substitutions (54, 55, 4, 56, and 57) are all well tolerated, in agreement with our hypothesis. Ethyl and 2,2,2-trifluoroethyl are the best substituents in terms of enzymatic, antibacterial, and specific activity. As active in *S. aureus* as the chloride (52) or *n*-propyl (4) substitutions, they display higher FabI specificity because they have no effect in *S. pneumoniae* at 64 μg/mL. Unsaturated groups such as trifluorovinyl (58) or *p*-tolyl (59) lose enzymatic and antibacterial activity, which

probably stems from their steric hindrance. Introduction of hydrophilic moieties in these side chains (60, 15, 61, 62, 63, and 64) also leads to activity losses, highlighting the lipophilic character of the left-part pocket. In view of these results, the ethyl group was further selected as our standard 4-position substitution on catechol.

In parallel, substitution on the right-part phenyl group was explored with a variety of short substituents displaying different stereoelectronic characteristics followed by the subsequent derivatization of the most promising ones (Table 2). Replacing the *p*-chloro group of triclosan with a methoxy group (65) without the *o*-chloro substituent is well tolerated, while moving the methoxy group to the meta position (66) is less favored. A meta acetamido substituent (67) also leads to a loss of enzymatic and antibacterial activity. At the para position, the electron-donating methoxy group (65) was exchanged by an electron-withdrawing methylsulfonyl group (68) that also retains *S. aureus* activity. A dioxolane moiety was then added to this methylsulfonyl group (69), which maintains antibacterial activity, indicating that space is available in this direction. Moving over to the ortho position, replacement of the *o*-chloro group of triclosan with an amino group (70) without the *p*-chloro substitution proves as potent on the enzyme. Adding a methyl moiety para to the aniline (71) or directly on the amino group (72), however, significantly decreases potency. Fluoride is also demonstrated to be a good ortho-substituting group,

Scheme 2. Synthesis of Table 2 Compounds<sup>a</sup>

<sup>a</sup>Reagents and conditions: (a) 4-methoxyphenylboronic acid, Cu(OAc)<sub>2</sub>, TEA, molecular sieves, DCM, rt (41%); (b) (i) *s*-BuLi, THF, 0 °C, (ii) 2-bromomethyl-1,3-dioxolane, THF, 0 °C to rt (quant); (c) 2-fluoronitrobenzene, KOH, ACN, 80 °C (quant); (d) H<sub>2</sub>, Pd/C, EtOH, rt (quant); (e) (i) Ac<sub>2</sub>O, HCO<sub>2</sub>H, 60 °C, (ii) **21**, THF, rt (quant); (f) BH<sub>3</sub>·Me<sub>2</sub>S, THF, 0 °C to reflux (quant); (g) NaNO<sub>2</sub>, AcOH, conc HCl, ACN, H<sub>2</sub>SO<sub>4</sub>, CuCl<sub>2</sub>, 0–50 °C (quant); (h) conc NH<sub>3</sub>, THF, 0 °C to rt (33%); (i) (i) propanaldehyde, MeOH, 30 °C, (ii) NaBH<sub>4</sub>, 30 °C (18%); (j) cyclopropanesulfonyl chloride, DCM, pyridine 0 °C to rt (quant); (k) TsCl, K<sub>2</sub>CO<sub>3</sub>, NaI, ACN, 70 °C (68%); (l) BBr<sub>3</sub>, DCM, –78 to –20 °C (41%); (m) BnBr, K<sub>2</sub>CO<sub>3</sub>, NaI, acetone, 40 °C (87%); (n) Mg, MeOH, rt (80%); (o) 3,4-difluoronitrobenzene, K<sub>2</sub>CO<sub>3</sub>, ACN, 80 °C (quant); (p) SnCl<sub>4</sub>, Et<sub>2</sub>O, HCl, 0 °C to rt (68%); (q) 3-bromo-1-propanol, K<sub>2</sub>CO<sub>3</sub>, DMF, microwave 180 °C (42%); (r) Pd(OH)<sub>2</sub>, ammonium formate, EtOH, 65 °C (45%); (s) benzyl chloroformate, THF, NaHCO<sub>3</sub>, 0 °C to rt (quant); (t) (i) *n*-BuLi, THF, –78 °C, (ii) racemic glycidyl butyrate, –78 °C to rt (quant); (u) MsCl, TEA, DCM, 0 °C to rt (42%); (v) (i) NaN<sub>3</sub>, DMF, 75 °C, (ii) H<sub>2</sub>, Pd/C, EtOAc, rt, (iii) H<sub>2</sub>, Pd/C, MeOH, rt (54%); (w) Ac<sub>2</sub>O, DCM, 0 °C to rt (55%); (x) 3',4'-difluoroacetophenone, KOH, DMF, 110 °C (quant); (y) BBr<sub>3</sub>, DCM, –78 °C to –20 °C (5%); (z) *O*-methylhydroxylamine, TEA, EtOH, rt (28%).

typically increasing *E. coli* enzymatic potency by a factor 5 (**73** vs **68**).

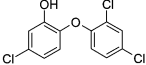
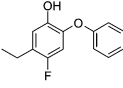
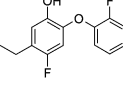
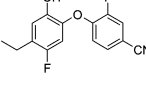
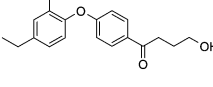
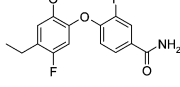
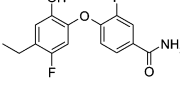
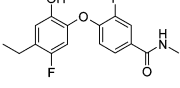
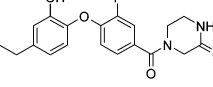
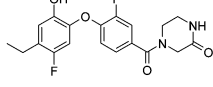
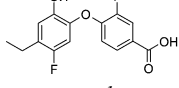
The para position was then revisited with an *o*-fluoride group. This led to a variety of well-tolerated substitutions, among them sulfonamides (**74**, **75**, **76**, and **77**), amines (**30** and **78**), inverted sulfonamides (**79**), carbonyl (**33**), and oxime (**34**). These groups generally conserve submicromolar *E. coli* enzymatic potency with the exception of **79** and **34** where the added steric bulk of the cyclopropyl group or the substituted oxime might prove deleterious. All these substitutions also display good antibacterial effect in *S. aureus*, indicating some degree of structural allowance at this location. This apparent permissiveness encouraged us to investigate the *p*-(acetylaminomethyl)-2-oxooxazolidin-3-yl substituent in the hope of restoring streptococci and enterococci activity by introducing to our FabI-targeted template an oxazolidinone pharmacophore.<sup>46</sup> However, this dual-mode attempt met with little

success, as the resulting compound (**32**) does not show such broadened spectrum and *S. aureus* antibacterial activity is even diminished.

The most active compounds on *S. aureus* from Table 2 (triclosan, **75**, and **33**) also turn out to display a biocidal effect, as testified by their MIC on *E. faecalis* or *S. pneumoniae*. Interestingly, these compounds are rather lipophilic (respective clogD according to ACDLabs V12.5: 5.2, 3.6, and 3.7), while more hydrophilic analogues such as **77** (clogD = 0.7) do not display an antibacterial effect in FabI independent strains. A similar observation can be made by comparing **78** (clogD = 3.8) that demonstrates the biocidal effect in *S. pneumoniae* to its FabI equipotent but more hydrophilic analogue **30** (clogD = 2.2), which does not.

These results prompted us to take a closer look at the clogD as a physicochemical parameter potentially linked to the biocidal character of our compounds. Enzymatic inhibition

Table 3. clogD and in Vitro Properties of Selected Derivatives

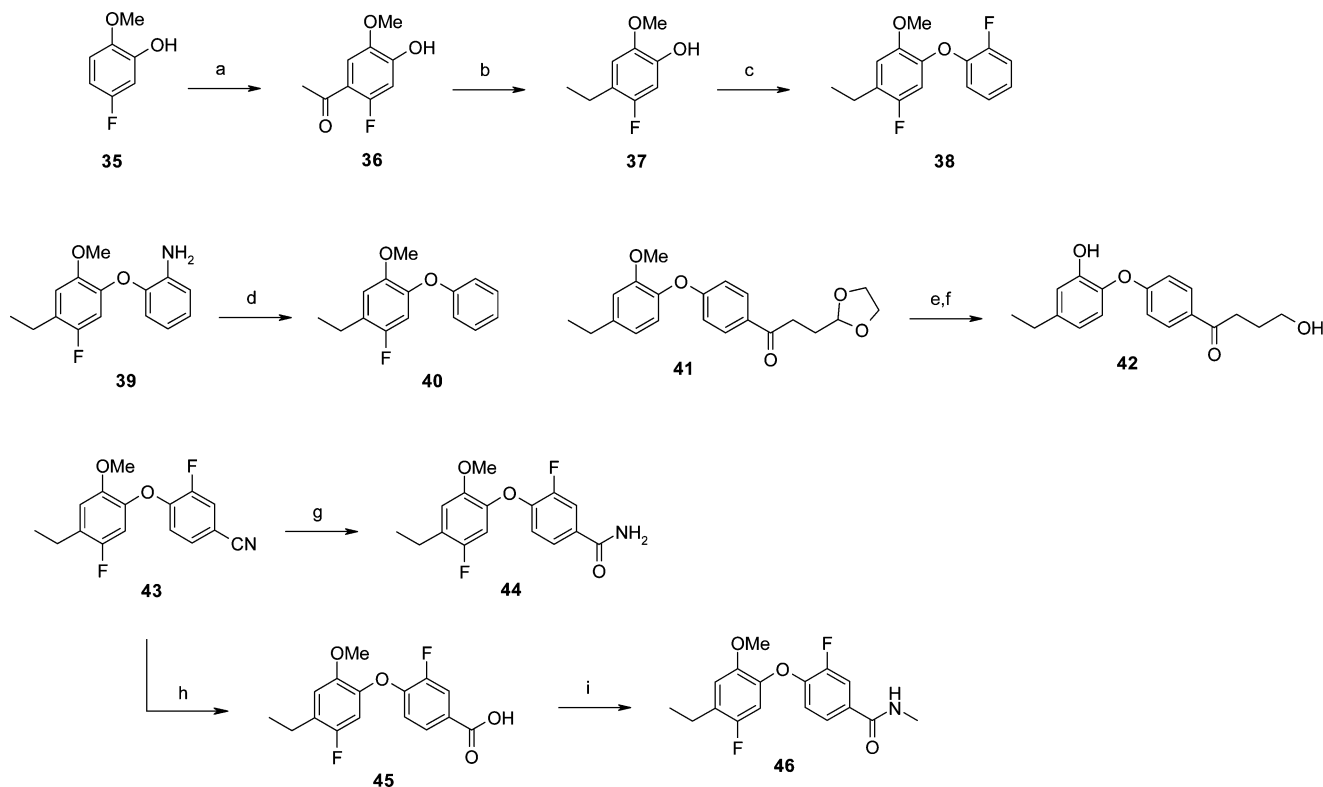
Compound	Structure	clogD <sup>a</sup>	IC <sub>50</sub> (μM)		MIC (μg/mL)			CYT <sup>f</sup>	
			<i>S. aureus</i> FabI	SAU <sup>b</sup>	ECO <sup>c</sup>	EFA <sup>d</sup>	SPN <sup>e</sup>	HepG2	
Triclosan		5.2	0.059	0.031	0.125	2	8	2	
80		4.1	0.037	0.062	1	32	16	16	
81		4.0	0.008	0.031	0.25	32	32	16	
82		3.4	0.031	0.062	1	32	8	16	
42		3.1	0.048	0.062	4	>32	16	16	
44		3.0	21	>32	>32	>32	>32	>32	
83		2.9	0.012	0.062	0.5	>32	>32	>32	
84		2.6	0.082	1	8	>32	>32	>32	
85		2.3	0.028	1	8	>32	>32	>32	
86		2.1	0.016	0.25	4	>32	>32	>32	
87		0.8	0.180	8	>32	>32	>32	>32	

<sup>a</sup>clogD calculated at pH 7.4 with ACDLabs V12.5. <sup>b</sup>SAU: *S. aureus* CIP54,146 (CRBIP Pasteur Institute). <sup>c</sup>ECO: *E. coli* K1 (O18:K1:H7, Robert Debré Hospital). <sup>d</sup>EFA: *E. faecalis* ATCC29212 (CRBIP Pasteur Institute). <sup>e</sup>SPN: *S. pneumoniae* D39 (Pasteur Institute). <sup>f</sup>Cytotoxicity ED<sub>50</sub> in μg/mL.

monitoring was also switched to *S. aureus* FabI to further increase the odds of optimization on staphylococci, although it was later realized that this series generally displays parallel inhibitory activity on both enzymes. During the course of our study, it soon became apparent that for our FabI-active compounds, clogD > 3 correlates to nonspecific biocidal effects monitored by activity on FabI-independent bacterial strains such as *E. faecalis* or *S. pneumoniae* and eukaryotic cells such as HepG2 (Table 3). As this biocidal effect increases with the clogD (triclosan with clogD > 5 displays the highest nonspecific effect of Table 3), so does the degree of lipophilicity surrounding the hydrophilic catechol group, therefore rendering the compounds amphiphilic. Since the nonspecific action of triclosan has been associated with membrane-destabilizing

effects,<sup>47–49</sup> we can surmise that the biocidal effects of its analogues are directly connected to their amphiphilic character. Our optimization rationale therefore focused on compounds displaying suitable polarity distribution to avoid amphiphilic properties and to bring their clogD below 3.

Since the *p*-acetyl group on the aromatic right-part represents a potent antistaphylococcal starting point (Table 2, compound 33), it was accordingly derivatized with hydrophilic moieties. The 4-hydroxybutyryl group (Table 3, compound 42) maintains the antibacterial effect in *S. aureus* but still displays some cytotoxicity. Further lowering the clogD by switching to amido or carboxylic moieties successfully phases out the nonspecific effect (Table 3, compounds 83, 84, 85, 86, and 87).

Scheme 3. Synthesis of Table 3 Compounds<sup>a</sup>

<sup>a</sup>Reagents and conditions: (a)  $\text{AcCl}$ ,  $\text{AlCl}_3$ , 1,2-dichloroethane, 40 °C (90%); (b)  $\text{Zn}$ ,  $\text{AcOH}$ , 70 °C (97%); (c) 1,2-difluorobenzene,  $\text{KOH}$ ,  $\text{DMSO}$ , 130 °C (10%); (d)  $\text{NaNO}_2$ ,  $\text{HBF}_4$ ,  $\text{AcOH}$ , rt (15%); (e)  $\text{BBr}_3$ ,  $\text{DCM}$ , -78 to -20 °C (17%); (f)  $\text{NaBH}_4$ ,  $\text{MeOH}$ , -78 to -5 °C (63%); (g)  $\text{CF}_3\text{CO}_2\text{H}$ ,  $\text{H}_2\text{SO}_4$  reflux (96%); (h)  $\text{NaOH}$ ,  $\text{MeOH}$ , reflux (87%); (i) (i)  $(\text{COCl})_2$ ,  $\text{DCM}$ , 0 °C to rt, (ii)  $\text{MeNH}_2$ ,  $\text{EtOH}$ , rt (quant).

Table 4. FabI Inhibition and Antibacterial Activity of 3-Pyridyl Right-Part Derivatives

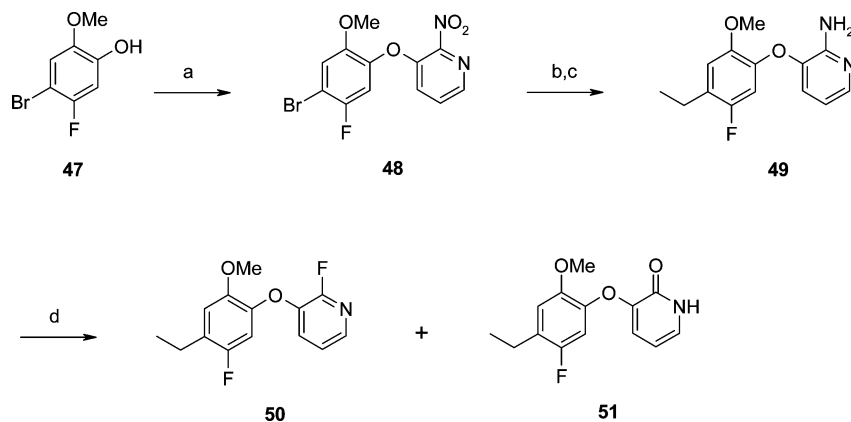
Compound	Structure	clogD <sup>a</sup>	IC <sub>50</sub> (μM)		MIC (μg/mL)		
			<i>S. aureus</i> FabI	SAU <sup>b</sup>	ECO <sup>c</sup>	EFA <sup>d</sup>	SPN <sup>e</sup>
94		1.7	0.056	0.5	0.25	>32	>32
95		1.9	>100	>32	>32	>32	>32
96		2.7	0.013	0.062	0.25	>32	>32

<sup>a</sup>clogD calculated at pH 7.4 with ACDLabs V12.5. <sup>b</sup>SAU: *S. aureus* CIP54,146 (CRBIP Pasteur Institute). <sup>c</sup>ECO: *E. coli* K1 (O18:K1:H7, Robert Debré Hospital). <sup>d</sup>EFA: *E. faecalis* ATCC29212 (CRBIP Pasteur Institute). <sup>e</sup>SPN: *S. pneumoniae* D39 (Pasteur Institute).

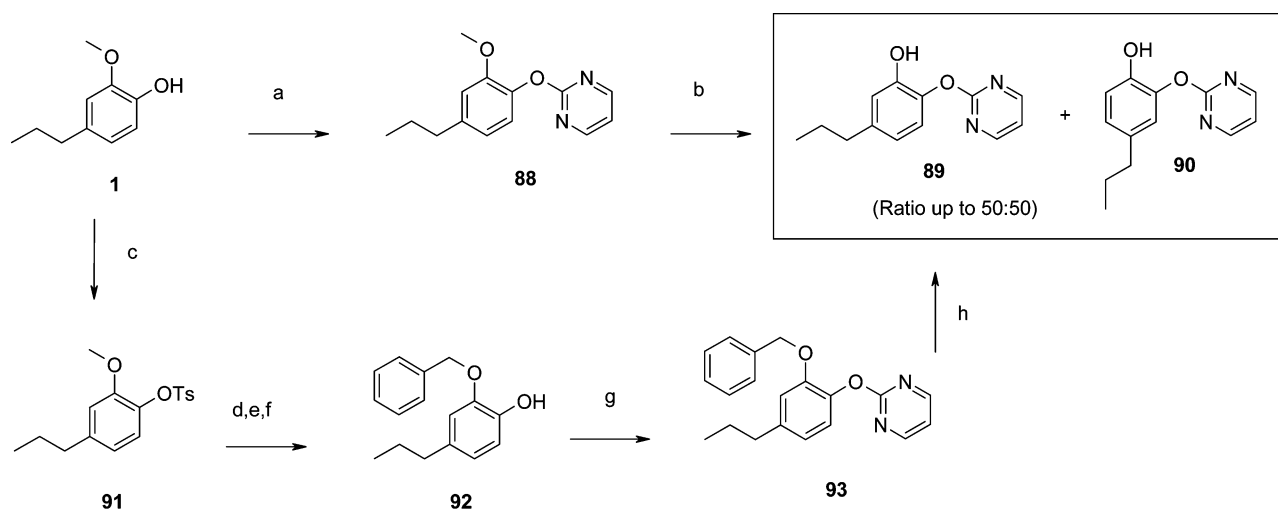
Triclosan is known to interact in its active site via strong hydrogen-bonding of its catechol hydroxyl with a conserved tyrosine residue and the 2'-hydroxyl of the cofactor (Figure 2 and reported costructures). Since removing this canonical interaction invariably leads to a loss of activity (44), a 4-fluoride group was introduced to the catechol with the objective of increasing this hydrogen-bonding. The reported  $\log K_{\text{HA}}$  for phenol is 1.66 vs 1.82 for *p*-fluorophenol, therefore demonstrating for the latter a slightly higher hydrogen-bond donation potential.<sup>50</sup> This *p*-fluorine introduction does not, however, affect much the  $\text{p}K_{\text{a}}$  of the catechol hydroxyl group.

For instance the calculated  $\text{p}K_{\text{a}}$  according to ACDLabs V12.5 for 83 is 8.93 ( $\pm 0.48$ ) vs 8.95 ( $\pm 0.35$ ) for its nonfluorinated catechol analogue, implying that in both cases the catechol hydroxyl group occurs mostly in its neutral form at pH 7.4. The addition of a *p*-fluoro group in our series indeed leads to a small improvement of enzymatic potency (86 vs 85), although one cannot rule out that this could also be imparted by the additional hydrophobic contact of this group with Phe 204 in the active site (Figure 3). Introduction of another fluoro group at the ortho-position of the right aryl moiety also improves enzymatic potency against *S. aureus* by a factor 5, as already



Scheme 4. Synthesis of Table 4 Compounds<sup>a</sup>

<sup>a</sup>Reagents and conditions: (a) 3-fluoro-2-nitropyridine, KOH, ACN, reflux (95%); (b) vinylboronic acid pinacol ester, Pd(PPh<sub>3</sub>)<sub>4</sub>, Cs<sub>2</sub>CO<sub>3</sub>, toluene reflux (76%); (c) H<sub>2</sub>, Pd/C, MeOH, rt (80%); (d) HBF<sub>4</sub>, NaNO<sub>2</sub>, AcOH, 0 °C (40% each).

Scheme 5. Regioisomerization Observed during the Deprotection of Electron-Deficient Right-Part Heteroaryls<sup>a</sup>

<sup>a</sup>Reagents and conditions: (a) 2-chloropyrimidine, K<sub>2</sub>CO<sub>3</sub>, ACN, 100 °C (60%); (b) BBr<sub>3</sub>, DCM, -78 °C to rt (quant); (c) TsCl, NaI, K<sub>2</sub>CO<sub>3</sub>, ACN, 70 °C (66%); (d) BBr<sub>3</sub>, DCM, -78 to -20 °C (65%); (e) BnBr, K<sub>2</sub>CO<sub>3</sub>, NaI, acetone, 40 °C (64%); (f) KOH, EtOH, water, reflux (86%); (g) 2-chloropyrimidine, K<sub>2</sub>CO<sub>3</sub>, ACN, 100 °C (54%); (h) H<sub>2</sub>, Pd/C, EtOH, rt (quant).

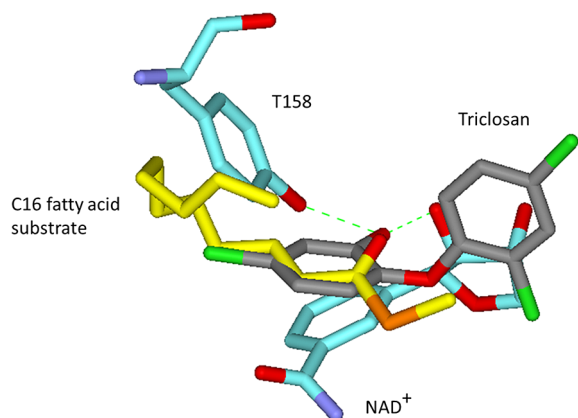


**Figure 2.** Overlay of triclosan (gray) with the crystal structure of a C16 fatty acid substrate (yellow) in InhA with its cofactor and Tyr 158 (blue).

observed on *E. coli* (Table 3, **81** vs **80** and Table 2, **73** vs **68**; vide infra for rationalization).

This optimization strategy led to some potent FabI-specific compounds, as testified by the amides **86** and **83**. Docking studies revealed **83** with possible binding conformation in the buried active site of *S. aureus* FabI delineated by key residues such as Tyr 147 and 157, Met 160, Ala 95 to Leu 102, Pro 192 to Ile 207, and the NADP<sup>+</sup> cofactor all along the bottom of the groove (Figure 3, for clarity Gly 200, Val 201, and Glu 202, which close the site, have been omitted). The ethyl group is in hydrophobic contact with the isopropyl group of Val 201 and the aromatic groups of Tyr 147 and Phe 204. The electron-rich catechol interacts through  $\pi$ -stacking with the electron-deficient pyridinium of NADP<sup>+</sup>, while the phenolic hydroxyl displays strong hydrogen-bond interactions with Tyr 157 and the 2'-hydroxyl of NADP's ribose. The second aryl group of **83** is in hydrophobic contact with Met 160. Its fluorine inserts in a small pocket shaped by a cluster of CH groups of NADP<sup>+</sup> in another hydrophobic contact that might explain the potency improvement between **80** and **81** (Table 3). Simultaneously, Ser 197 pushes this fluoride group away, which helps direct the aryl group toward a nice chelation of the enzyme by hydrogen-bonding with the carbonyl and amide hydrogen of Ala 97

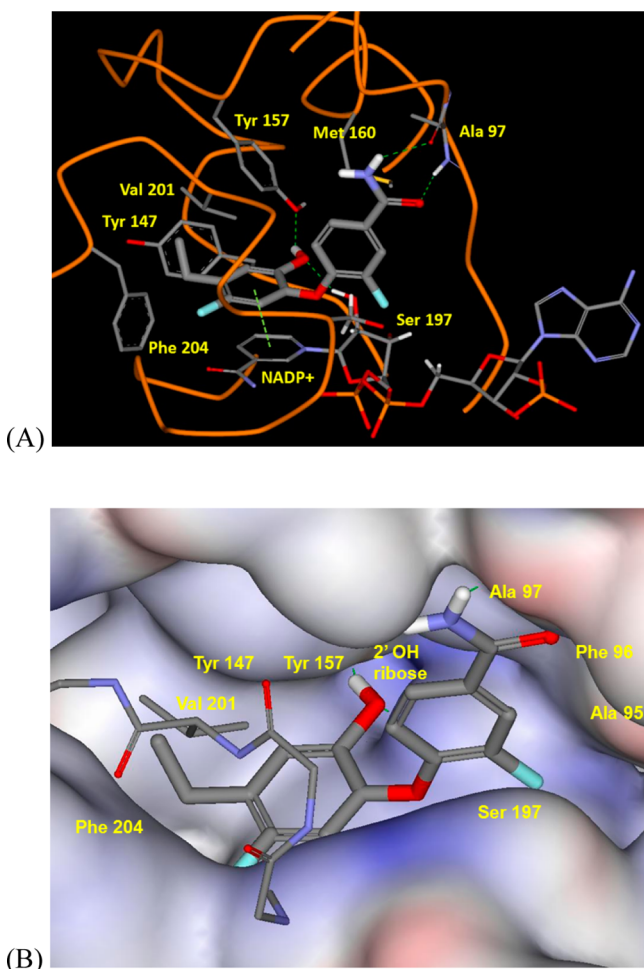


**Figure 3.** Compound **83** (bold) docked in the active site of *S. aureus* FabI using Flo+.<sup>51</sup> (A) Protein is displayed as orange wire with detailed key residues and NADP<sup>+</sup> in stick style. (B) Protein and NADP<sup>+</sup> are displayed as electrostatic surfaces. For clarity purposes, Val 201 is in stick style.

(Figure 3). Introducing a methyl group to the amide would result in loss of the hydrogen-bonding to Ala 97 due to the preferential trans rotamer, therefore providing a possible explanation for the weaker enzymatic activity of **84** vs **83** (Table 3).

Replacement of the right aryl ring with heteroaryl groups can constitute another way of lowering the clogD of our compounds below the threshold of 3. However, it was observed that for a variety of heterocycles (among which are 2-pyrimidyl, 2-pyridyl, 2-quinolyl) this was not a viable option because of the self-isomerization encountered with these products. For instance, independent of the final deprotection procedure, catechols **89** and **90** are isolated in a ratio close to 50:50 (Scheme 5). Moreover, their separation by HPLC followed by concentration also leads to reisolated mixtures. This intrinsic stability issue could be explained by a Smiles rearrangement at the electron-deficient heteroaryl carbon bearing the catechol group.

To avoid this regioisomerization problem, 3-pyridyl heterocycles with less electron-withdrawing character at the carbon bearing the catechol were synthesized. Satisfyingly, the resulting compounds turn out to be stable and display clogD < 3 without any sign of biocidal effect (Table 4). Derivative **94** retains FabI potency, which might be explained by hydrogen-bonding of its

*o*-amino group with the carbonyl of Ala95. On the contrary, pyridone **95** loses all potency, presumably because of electronic repulsion with the carbonyl of Ala95. Introducing the beneficial hydrophobic *o*-fluoro group leads to 3-pyridyl **96**, which displays similar levels of activity as the best right-part aromatic derivatives.

Among the most active compounds, **83** is a specific, potent FabI inhibitor. **83** synergizes strongly with the cofactor NADPH against *S. aureus* FabI (Figure 4), whereas NADP<sup>+</sup>

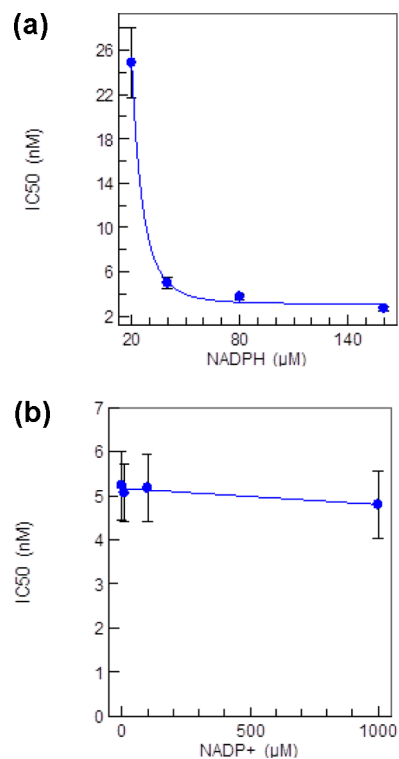


**Figure 4.** (a) Influence of NADPH on the IC<sub>50</sub> of **83** against FabI of *S. aureus* (NADP<sup>+</sup> = 0 μM). (b) Influence of NADP<sup>+</sup> on the IC<sub>50</sub> of **83** against FabI of *S. aureus* (NADPH = 40 μM).

does not up to 1 mM. The postulated binding mode of this compound involving a  $\pi$ -stacking with the electron-deficient pyridinium of NADP<sup>+</sup> is therefore challenged by this observation and needs further explanation. As shown in Figure 5, a slow onset of inhibition is observed with **83**. Interestingly,

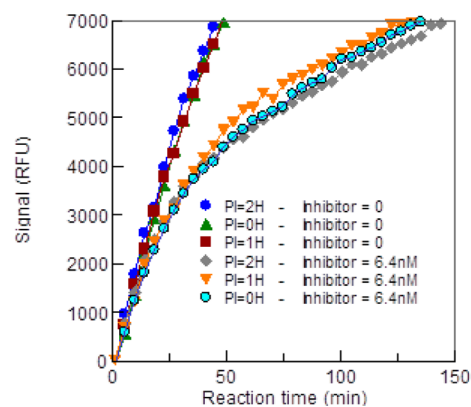


**Figure 5.** Influence of the preincubation time on *S. aureus* FabI inhibition kinetics of **83**.

slow inhibition kinetics is not significantly modified by the preincubation time (0–2 h) between FabI, **83**, and NADPH. These three partners are therefore not sufficient for the onset of full FabI inhibition: the addition of the fatty acid t-o-NAC-thioester (*trans*-2-octenoyl *N*-acetylcysteamine thioester) substrate, which allows enzyme catalysis to start, was the triggering event here. As the addition of t-o-NAC-thioester leads to the oxidation of NADPH to NADP<sup>+</sup>, it is tempting to speculate the next events: reduced t-o-NAC-thioester could leave the active site more rapidly than NADP<sup>+</sup> and be replaced by **83**, thus building a more stable ternary complex in agreement with the postulated  $\pi$ -stacking mode of binding of our inhibitor. The fact that NADP<sup>+</sup> itself does not synergize at all with **83** would imply that FabI's native conformation is a very poor binder of NADP<sup>+</sup>, since this oxidized cofactor could actually be more efficiently trapped in a catalytically active conformation. At this stage, additional investigations would be required to understand and validate the nature of this inhibition mechanism.

When compared to linezolid, a drug currently approved for nosocomial pneumonia as well as complicated skin and skin structure infections caused by *S. aureus* (methicillin-susceptible and -resistant strains), **83** displays highly potent in vitro antistaphylococcal activities (Table 5), with a low frequency of

**Table 5.** MIC<sub>90</sub> ( $\mu\text{g/mL}$ ) of **83** and Linezolid against Staphylococci

compd	community-acquired MRSA <sup>a</sup> (30) <sup>f</sup>	NARSA MRSA <sup>b</sup> (48) <sup>f</sup>	MSSA <sup>c</sup> (40) <sup>f</sup>	MRSE <sup>d</sup> (30) <sup>f</sup>	MRSH <sup>e</sup> (30) <sup>f</sup>
<b>83</b>	$\leq 0.03$	0.12	0.06	2	0.5
linezolid	2	$\geq 16$	2	1	1

<sup>a</sup>Methicillin resistant *S. aureus*. <sup>b</sup>Network on antimicrobial resistance in *S. aureus*. <sup>c</sup>Methicillin susceptible *S. aureus*. <sup>d</sup>Methicillin resistant *S. epidermidis*. <sup>e</sup>Methicillin resistant *S. hemolyticus*. <sup>f</sup>Number of isolates.

spontaneous resistance, between  $2.5 \times 10^{-9}$  and  $7 \times 10^{-9}$  at 4 times the MIC.<sup>52</sup> In addition to its strong potency against staphylococci, this compound displays good potential against some FabI-dependent Gram-negative bacteria (Table 6). Promising activities have also been reported on *Chlamydomytila pneumoniae*, *Helicobacter pylori*, and *Acinetobacter baumannii*.<sup>53</sup>

Preclinical studies on **83** showed that it demonstrates moderate thermodynamic aqueous solubility: around 0.02 mg/mL at pH 7.4. Its solubility could be increased to 11.3 mg/mL in an aqueous solution of 20% hydroxypropyl- $\beta$ -cyclodextrin (HPBCD) and 1–5% glucose. This compound displays high in vitro affinity for human serum albumin (95%) and weak inhibition of cytochromes P450.<sup>54</sup> Toxicology evaluation of **83** was performed following single intravenous dosing in rats and mice and twice daily intravenous dosing in rats and dogs for 14 days. Single dose toxicity studies in mice and rats showed that the maximum tolerated dose (MTD) was greater than 200 mg/kg. In the rat 2-week study, the no observed adverse effect level (NOAEL) was 200 mg kg<sup>-1</sup> day<sup>-1</sup>

without significant clinical findings on macroscopic or microscopic examinations. In dogs, the NOAEL was decreased at 100 mg kg<sup>-1</sup> day<sup>-1</sup> because of a significant body weight loss in only one female. In safety pharmacology studies, **83** administered in rats as single intravenous injections up to 200 mg/kg did not display any relevant clinical signs related to the compound, with no reported potential effects on the central nervous system or on respiratory functions. Single intravenous infusions up to 100 mg/kg in beagle dogs were also devoid of observable clinical signs related to the compound, with no reported potential effects on cardiovascular functions and no QT prolongation. Overall, the results from these toxicology and safety pharmacology studies show no findings that should prevent **83** from progressing to human studies.<sup>55</sup> In pharmacokinetic studies in rats, **83** displayed a high plasma clearance of 6.4 L h<sup>-1</sup> kg<sup>-1</sup>, as could be expected from the metabolic lability of the phenolic moiety.<sup>56</sup> Nevertheless high concentrations of compound were achieved in all tested tissues (Table 7).

The in vivo efficacy of **83** was then evaluated using murine infection models. In a systemic model of lethal infection of mice with an intraperitoneal challenge of MRSA, the ED<sub>50</sub> of the compound was determined as the single subcutaneous dose administered 5 min after the infection that provided 50% survival of treated animals at 48 h postinfection (Table 8). These results demonstrate a good protective action against a variety of multiresistant *S. aureus*. Additional in vitro and in vivo data about **83** have already been reported,<sup>53</sup> which helps further validate FabI as a suitable antibiotic target on *S. aureus*. In light of these promising results, as well as its good preclinical safety dossier and low cost-of-goods, **83** has been selected for clinical development.

To help establish human doses, a PK/PD investigation of **83** was performed against *S. aureus* in an in vitro one compartment pharmacodynamic model. Regimens of 600, 900, and 1200 mg q6h or q8h with a prolonged infusion of 2 h were found to achieve the greatest efficacy against MRSA USA300, with rapid and sustainable killing activity. In this study, **83** demonstrated a dose-dependent response using fAUC/MIC and %T/MIC as the predictive pharmacodynamic parameters.<sup>57</sup> No relevant clinical or laboratory findings related to **83** were reported in healthy human volunteers at these doses, which supports further clinical development.<sup>58,59</sup>

## CONCLUSION

Starting from triclosan as a lead, we have described some elements of our optimization program to decouple its specific FabI effect from its nonspecific cytotoxic component. This strategy was successfully implemented to deliver highly specific and potent FabI inhibitors, among which is **83**, a novel antibacterial compound active against resistant staphylococci and some clinically relevant Gram negative bacteria. We also report murine in vivo efficacy data, which help further validate FabI as a suitable antibiotic target on *S. aureus*. In hopes of exploitation of its untapped mode of action, **83** is currently

**Table 6.** MIC<sub>90</sub> ( $\mu\text{g/mL}$ ) of **83** and Levofloxacin against Gram-Negative Bacteria

compd	<i>Neisseria gonorrhoeae</i> (10) <sup>a</sup>	<i>Neisseria meningitidis</i> (10) <sup>a</sup>	<i>Haemophilus influenzae</i> (30) <sup>a</sup>	<i>Moraxella catarrhalis</i> (20) <sup>a</sup>	<i>Escherichia coli</i> (30) <sup>a</sup>	<i>Proteus mirabilis</i> (10) <sup>a</sup>
<b>83</b>	0.25	0.25	0.5	2	1	2
levofloxacin	0.5	$\leq 0.008$	0.03	0.03	$\geq 16$	0.06

<sup>a</sup>Number of isolates.

Table 7. Rat Pharmacokinetic Data for Compound 83<sup>a</sup>

	plasma	liver	kidney	brain	heart	lung
C <sub>max</sub> (ng/g)	30436 <sup>b</sup>	51700	63000	37800	42100	28900
AUC <sub>(0-∞)</sub> (ng·h/mL)	13936	105067	20262	27635	23920	18393
T <sub>1/2</sub> <sup>c</sup> (h)	4.9	9.2	8.5	4.2	5	5.9

<sup>a</sup>Female Sprague–Dawley rats dosed iv, 2 × 50 mg/kg. <sup>b</sup>ng/mL. <sup>c</sup>Terminal elimination half-life.

Table 8. In Vivo Activity of 83 in a Murine Systemic Infection Model<sup>a</sup>

<i>S. aureus</i> strain	83 MIC (μg/mL)	83 mean ED <sub>50</sub> (mg/kg) (CI) <sup>b</sup>	vancomycin mean ED <sub>50</sub> (mg/kg) (CI) <sup>b</sup>
MRSA NRS382 (USA100)	0.06	19.3 (12.5–28.5)	6.0 (1.8–12.4)
MRSA NRS384 (USA300)	0.06	45.1 (33.4–50.6)	9.4 (9.4–9.4)
MRSA NRS385 (USA500)	0.06	28.3 (21.0–38.2)	5.0 (1.9–9.8)

<sup>a</sup>Female Swiss mice (6 per group). <sup>b</sup>Numbers in parentheses are 95% confidence ranges.

undergoing clinical development for the treatment of severe bacterial infections in human.

## EXPERIMENTAL SECTION

**FabI *E. coli* Enzyme Assay.** Compound inhibitory activity of FabI enzyme was measured in vitro by IC<sub>50</sub> determination using a fluorescent based assay. The protein FabI from *E. coli* was prepared and purified using standard methods for recombinant protein expression after cloning of the gene in a prokaryotic expression vector. The biochemical activity of the FabI enzyme was assessed using the following method. The assay buffer “AB” contained 50 mM Hepes, pH 7.5, 100 μM dithiothreitol, and 0.006% Triton-X100. The following components were added in a black polystyrene Costar plate to a final volume of 55 μL: 1.5 μL DMSO, or inhibitor dissolved in DMSO and 53.5 μL of a FabI/NADH/NAD<sup>+</sup> mixture in AB. After 90 min of preincubation at room temperature, the reaction was initiated by addition of 5 μL of crotonoyl-CoA to a final volume of 60 μL. This reaction mixture was then composed of 40 nM FabI (produced in house from *E. coli*, C-terminal 6-His tagged), 20 μM NADH (Biochemika), 10 μM NAD<sup>+</sup> (Biochemika), 50 μM crotonoyl-CoA (Biochemika), and compound at defined concentration. Fluorescence intensity of NADH (λ<sub>ex</sub> = 360 nm, λ<sub>em</sub> = 520 nm) was measured immediately after crotonoyl-CoA addition, and 2 h later by a Fluostar Optima (BMG). Enzyme activity is proportional to the signal decrease from which inhibition percentages are derived. For IC<sub>50</sub> determinations, the inhibitor was tested at 6–10 different concentrations, and the related inhibitions were fitted to a classical Langmuir equilibrium model using XLFIT (IDBS).

**FabI *S. aureus* Enzyme Assay.** Compound inhibitory activity of FabI enzyme was measured in vitro by IC<sub>50</sub> determination using a fluorescence based assay. The protein FabI from *S. aureus* was prepared and purified using standard methods for recombinant protein expression after cloning of the gene in a prokaryotic expression vector. The biochemical activity of the FabI enzyme was assessed using the following method. The assay buffer “AB” contained 50 mM ADA (N-(2-acetamido)iminodiacetic acid monosodium salt), pH 6.5, 1 mM dithiothreitol, 0.006% Triton-X100, and 50 mM NaCl. The following components were added in a white polystyrene Costar plate (ref 3912) to a final volume of 55.5 μL: 1.5 μL DMSO or inhibitor dissolved in DMSO and 54 μL of a FabI/NADPH/NADP<sup>+</sup> mixture in AB. After 60 min of preincubation at room temperature, the reaction was started by addition of 5 μL of *trans*-2-octenoyl *N*-acetylcysteamine thioester (*t*-o-NAC) to a final volume of 60.5 μL. This reaction mixture was then composed of 2 nM FabI, 40 μM NADPH (Sigma, N7505), 10 μM NADP<sup>+</sup> (Sigma, N5755), 100 μM *t*-o-NAC, and compound at defined concentration. Fluorescence intensity of NADPH (λ<sub>ex</sub> = 360 nm, λ<sub>em</sub> =

520 nm) was measured immediately after *t*-o-NAC addition (*T*<sub>0</sub>), and approximately 50 min later (*T*<sub>50</sub>) by a Fluostar Optima (BMG) to achieve ±30% of NADPH conversion. Enzyme activity was calculated by first subtracting the *T*<sub>0</sub> signal from the *T*<sub>50</sub> and then subtracting background signal (FabI = 0). Percentages of inhibition were calculated against untreated samples (inhibitor = 0), and IC<sub>50</sub> values were fitted to a classical Langmuir equilibrium model using XLFIT (IDBS).

**Antibacterial Activity Assay.** Whole-cell antimicrobial activity was determined by broth microdilution method in microtiter plates according to CLSI guidelines. The compound was assayed in serial 2-fold dilutions ranging from 0.06 to 64 μg/mL. Test organisms were selected from the following laboratory strains: *Staphylococcus aureus* CIP54.146, *Escherichia coli* K1 Robert Debré Hospital, Paris, France, *E. faecalis* ATCC29212, *S. pneumoniae* D39 Pasteur Institute, Paris, France. Bacteria were grown in cation-adjusted Mueller–Hinton broth (ca-MHB) using an inoculum of 5 × 10<sup>5</sup> CFU/mL incubated at 35 °C for 18 h unless otherwise stated. For *S. pneumoniae*, ca-MHB was supplemented with 2.5% lysed horse blood, and growth was performed in 5% CO<sub>2</sub>. The minimum inhibitory concentration (MIC) was defined as the lowest concentration of compound at which no visible bacterial growth was observed.

**Docking Method.** Compound 83 was docked in the *S. aureus* FabI active site using the MCDock module with standard parameters (QXP Flo+)<sup>51</sup> and the deposited structure 3GR6. Key residues Tyr 147 and 157, Met 160, Ala 95 to Leu 102, Pro 192 to Ile 207 as well as the NADP<sup>+</sup> cofactor were allowed to be flexible while the rest of the active site was kept rigid.

**General Experimental.** All reactions were carried out under an inert (nitrogen or argon) atmosphere unless indicated otherwise. Starting materials, reagents, and solvents were obtained from commercial sources and were used without further purification unless otherwise specified. Celite is a filter aid composed of diatomaceous silica and is a registered trademark of Celite Corporation. Analtech silica gel GF and E. Merck silica gel 60 F-254 thin layer plates were used for thin layer chromatography. Flash chromatography was carried out on Flashsmart Pack cartridge irregular silica 40–60 μm or spherical silica 20–40 μm. Preparative thin layer chromatography was carried out on Analtech silica gel GF 1000 μm, 20 cm × 20 cm. Yields refer to purified products and are not optimized. All new compounds gave satisfactory analytical data. <sup>1</sup>H NMR spectra were recorded at 300 or 400 MHz on a Bruker instrument, and chemical shifts are reported in parts per million (δ) downfield from the internal standard tetramethylsilane. Mass spectra were obtained using electrospray (ESI) ionization techniques on an Agilent 1100 series LCMS instrument. HPLC (analytical and preparative) were performed on an Agilent 1100 HPLC instrument with diode array detection. Preparative HPLC was performed at 0.7 mL/min on a Thermo Electron, Hypersil BDS C-18 column (250 mm × 4.6 mm, 5 μm) using a gradient of acetonitrile and water with 0.1% TFA (50% in acetonitrile to 100% and then back to 50%). The tested compounds were determined to be >95% pure via HPLC.

**General Procedure for the Synthesis of (4-Ethyl-5-fluoro-2-hydroxyphenoxy)-Based Compounds of Table 3 As Illustrated by Synthesis of 4-(4-Ethyl-5-fluoro-2-hydroxyphenoxy)-3-fluorobenzamide (83).** 1-(2-Fluoro-4-hydroxy-5-methoxyphenyl)ethanone (36). To a suspension of aluminum chloride (1.17g, 8.79 mmol) in 1,2-dichloroethane (2 mL) was added acetyl chloride (0.55g, 7.03 mmol). After the mixture was stirred for 10 min, a solution of 5-fluoro-2-methoxyphenol 35 (0.50g, 3.52 mmol) in 1,2-dichloroethane (2 mL) was added dropwise. The reaction mixture was stirred

overnight at 40 °C. The mixture was then poured on ice–water and extracted with diethyl ether. The organic phases were combined, washed with brine, dried over sodium sulfate, and concentrated to afford 582 mg (90%) of the title compound as an off-white solid. MS (ES) *m/e* 185 (M + H)<sup>+</sup>. TLC: eluent cyclohexane/EtOAc, 7/3, *R<sub>f</sub>* = 0.23.

**4-Ethyl-5-fluoroguaiacol (37).** A solution of 36 (18.0 g, 97.7 mmol) in glacial acetic acid (800 mL) is stirred at 70 °C before adding added zinc dust (63.9 g, 977 mmol). The resulting gray heterogeneous mixture is then heated at reflux and stirred overnight using a mechanical stirrer. After this period, zinc has aggregated and conversion rate reaches 90% according to the <sup>1</sup>H NMR analysis of a crude aliquot. Therefore, the zinc metal is removed by filtration on a fritted glass, and fresh zinc dust (6.4 g, 98 mmol) is added to the resulting limpid yellow filtrate. The solution is heated at reflux overnight until completion of the reaction. The solution is filtered on a fritted glass and basified until pH 11–12 is reached with a saturated aqueous solution of potassium carbonate (1.5 L) and with additional solid potassium carbonate if needed. The resulting aqueous layer is then extracted with ethyl acetate (1.0 L), dried over sodium sulfate or by azeotropic toluene distillation, filtered, and concentrated under vacuum to afford the pure title compound (16.1 g, 94.7 mmol, 97%) as a pale yellow oil. The title compound is a volatile product and should be kept in the refrigerator under argon away from light (darkens with oxygen and/or UV exposure). No or weak response in MS. <sup>1</sup>H NMR (DMSO),  $\delta$  (ppm): 9.20 (bs, 1H), 6.78 (d, *J* = 3.6 Hz, 1H), 6.54 (d, *J* = 9 Hz, 1H), 3.73 (s, 3H), 2.50 (q, *J* = 7.2 Hz, 2H), 1.12 (t, *J* = 7.4 Hz, 3H).

**4-(4-Ethyl-5-fluoro-2-methoxyphenoxy)-3-fluorobenzonitrile (43).** To a solution of 37 (8 g, 47 mmol) and 3,4-difluorobenzonitrile (6.53 g, 47 mmol) in 80 mL of anhydrous acetonitrile is added potassium hydroxide (3.15 g, 56.4 mmol). The reaction mixture under argon atmosphere is stirred under reflux for 16 h. Concentration, addition of a saturated aqueous solution of ammonium chloride (100 mL), extraction with ethyl acetate (2 × 25 mL), reunification of the organic phases, brine wash, drying over sodium sulfate, and final concentration affords 12.95 g (95%) of the title compound as a brown solid, which was used as such for the next step. MS (ES) *m/e* 290 (M + H)<sup>+</sup>. TLC: eluent cyclohexane/EtOAc, 7/3, *R<sub>f</sub>* = 0.74.

**4-(4-Ethyl-5-fluoro-2-methoxyphenoxy)-3-fluorobenzamide (44).** To 43 (12.95 g, 7.05 mmol) are added trifluoroacetic acid (52 mL) and concentrated sulfuric acid (13 mL). After 1 h and 30 min under reflux the reaction mixture is cooled to room temperature and then poured into ice–water (400 mL). Dichloromethane extraction (100 mL, then 2 × 25 mL), reunification of the organic phases, saturated aqueous sodium hydrogenocarbonate wash (250 mL, pH 8–8.5), drying over sodium sulfate, and final concentration affords 13.31 g (96%) of the title compound as an off-white solid. MS (ES) *m/e* 294 (M + H)<sup>+</sup>. TLC: eluent dichloromethane/methanol, 9/1, *R<sub>f</sub>* = 0.3. <sup>1</sup>H NMR (DMSO)  $\delta$  (ppm): 7.96 (bs, 1H), 7.82 (d, *J* = 12.1 Hz, 1H), 7.64 (d, *J* = 8.3 Hz, 1H), 7.41 (bs, 1H), 7.13 (d, *J* = 7.2 Hz, 1H), 7.04 (d, *J* = 10.0 Hz, 1H), 6.80 (t, *J* = 8.5 Hz, 1H), 3.73 (s, 3H), 2.64 (q, *J* = 7.6 Hz, 2H), 1.22 (t, *J* = 7.5 Hz, 3H).

**4-(4-Ethyl-5-fluoro-2-hydroxyphenoxy)-3-fluorobenzamide (83).** To 44 (13.31 g, 4.59 mmol) in 130 mL of dichloromethane under argon at –78 °C under intense stirring is added, over 15–20 min, boron tribromide (130 mL at 1 M in dichloromethane). The reaction mixture is warmed to room temperature under stirring and after 3 h is cooled back to –20 °C for quenching with a saturated aqueous solution of ammonium chloride (100 mL). Partial concentration is performed to remove 170 mL of dichloromethane. An amount of 100 mL of ethyl acetate is added. Extraction of the aqueous phase (2 × 25 mL of ethyl acetate), reunification of the organic phases, aqueous sodium hydrogenocarbonate (200 mL at 1 N) wash, drying over sodium sulfate, and final concentration afford the crude material which is purified on silica gel (gradient dichloromethane/methanol, 100/0 → 95/5) to afford the title compound, 8.75g (68%). MS (ES) *m/e* 294 (M + H)<sup>+</sup>. TLC: eluent dichloromethane/methanol, 20/1, *R<sub>f</sub>* = 0.4. <sup>1</sup>H NMR (DMSO)  $\delta$  (ppm): 9.59 (s, 1H, OH), 7.95 (bs, 1H, NH), 7.80 (d, 1H, *J* = 12.2 Hz), 7.63 (d, 1H, *J* = 8.3 Hz), 7.40 (bs, 1H, NH), 6.96

(d, 1H, *J* = 9.8 Hz), 6.87 (d, 1H, *J* = 7.9 Hz), 6.78 (t, 1H, *J* = 8.2 Hz), 2.56 (q, 2H, *J* = 7.4 Hz), 1.17 (t, 3H, *J* = 7.3 Hz).

## ■ ASSOCIATED CONTENT

### Supporting Information

Synthetic procedures and spectroscopic details for all final compounds. This material is available free of charge via the Internet at <http://pubs.acs.org>.

## ■ AUTHOR INFORMATION

### Corresponding Author

\*Phone: +33-157140522. Fax: +33-157140524. E-mail: [vincent.gerusz@mutabilis.fr](mailto:vincent.gerusz@mutabilis.fr).

### Present Addresses

<sup>§</sup>GlaxoSmithKline, 25-27 Avenue du Québec, 91951 Les Ulis, France.

<sup>||</sup>Galapagos, 102 Avenue Gaston Roussel, 93230 Romainville, France.

<sup>†</sup>ESE Conseil, 66 Boulevard Senard, 92210 Saint Cloud, France.

<sup>#</sup>Alderys, 86 Rue de Paris, 91400 Orsay, France.

<sup>∞</sup>FAB Pharma, 11 Avenue Myron Herrick, 75008 Paris, France.

### Notes

The authors declare no competing financial interest.

## ■ ACKNOWLEDGMENTS

The authors gratefully thank Drs. André Bryskier and Stefan Fischer for enlightening discussions on these topics, as well as the Robert Debré Hospital and the Pasteur Institute for providing *S. pneumoniae* D39 and *E. coli* strains. This work has been partly supported by Grants I06-222/R and I09-1739/R from the Medicen Paris Region Competitiveness Cluster and the Seine-Saint-Denis County.

## ■ REFERENCES

- (1) Furtado, G. H.; Nicolau, D. P. Overview perspective of bacterial resistance. *Expert Opin. Ther. Pat.* **2010**, *20*, 1273–1276.
- (2) Boucher, H. W.; Talbot, G. H.; Bradley, J. S.; Edwards, J. E.; Gilbert, D.; Rice, L. B.; Scheld, M.; Spellberg, B.; Bartlett, J. Bad bugs, no drugs: no ESCAPE! An update from the Infectious Diseases Society of America. *Clin. Infect. Dis.* **2009**, *48*, 1–12.
- (3) Chambers, H. F.; Deleo, F. R. Waves of resistance: *Staphylococcus aureus* in the antibiotic era. *Nat. Rev. Microbiol.* **2009**, *7*, 629–641.
- (4) Dulon, M.; Haamann, F.; Peters, C.; Schablon, A.; Nienhaus, A. MRSA prevalence in European healthcare settings: a review. *BMC Infect. Dis.* **2011**, *11*, 138.
- (5) Watkins, R. R.; David, M. Z.; Salata, R. A. Current concepts on the virulence mechanisms of methicillin-resistant *Staphylococcus aureus*. *J. Med. Microbiol.* **2012**, *61*, 1179–1193.
- (6) Zhang, Y. M.; White, S. W.; Rock, C. O. Inhibiting bacterial fatty acid synthesis. *J. Biol. Chem.* **2006**, *281*, 17541–17544.
- (7) Wright, H. T.; Reynolds, K. A. Antibacterial targets in fatty acid biosynthesis. *Curr. Opin. Microbiol.* **2007**, *10*, 447–453.
- (8) Brinster, S.; Lamberet, G.; Staels, B.; Trieu-Cuot, P.; Gruss, A.; Poyart, C. Type II fatty acid synthesis is not a suitable antibiotic target for Gram-positive pathogens. *Nature* **2009**, *458*, 83–86.
- (9) Brinster, S.; Lamberet, G.; Staels, B.; Trieu-Cuot, P.; Gruss, A.; Poyart, C. *Nature* **2010**, *463*, E4.
- (10) Balemans, W.; Lounis, N.; Gilissen, R.; Guillemont, J.; Simmen, K.; Andries, K.; Koul, A. *Nature* **2010**, *463*, E3 ; discussion E4.
- (11) Parsons, J. B.; Rock, C. O. Is bacterial fatty acid synthesis a valid target for antibacterial drug discovery? *Curr. Opin. Microbiol.* **2011**, *14*, 544–549.
- (12) Parsons, J. B.; Frank, M. W.; Subramanian, C.; Saenkham, P.; Rock, C. O. Metabolic basis for the differential susceptibility of Gram-

positive pathogens to fatty acid synthesis inhibitors. *Proc. Natl. Acad. Sci. U.S.A.* **2011**, *108*, 15378–15383.

(13) Gerusz, V. Recent advances in the inhibition of bacterial fatty acid biosynthesis. *Annu. Rep. Med. Chem.* **2010**, *45*, 295–311.

(14) Heath, R. J.; Li, J.; Roland, G. E.; Rock, C. O. Inhibition of the *Staphylococcus aureus* NADPH-dependent enoyl-acyl carrier protein reductase by triclosan and hexachlorophene. *J. Biol. Chem.* **2000**, *275*, 4654–4659.

(15) Heath, R. J.; Rock, C. O. Enoyl-acyl carrier protein reductase (fabI) plays a determinant role in completing cycles of fatty acid elongation in *Escherichia coli*. *J. Biol. Chem.* **1995**, *270*, 26538–26542.

(16) Banerjee, A.; Dubnau, E.; Quemard, A.; Balasubramanian, V.; Um, K. S.; Wilson, T.; Collins, D.; de Lisle, G.; Jacobs, W. R., Jr. InhA, a gene encoding a target for isoniazid and ethionamide in *Mycobacterium tuberculosis*. *Science* **1994**, *263*, 227–230.

(17) Quémard, A.; Sacchettini, J. C.; Dessen, A.; Vilcheze, C.; Bittman, R.; Jacobs, W. R., Jr.; Blanchard, J. S. Enzymatic characterization of the target for isoniazid in *Mycobacterium tuberculosis*. *Biochemistry* **1995**, *34*, 8235–8241.

(18) Lu, H.; Tonge, P. J. Inhibitors of FabI, an enzyme drug target in the bacterial fatty acid biosynthesis pathway. *Acc. Chem. Res.* **2008**, *41*, 11–20.

(19) Baldock, C.; Rafferty, J. B.; Sedelnikova, S. E.; Baker, P. J.; Stuitje, A. R.; Slabas, A. R.; Hawkes, T. R.; Rice, D. W. A mechanism of drug action revealed by structural studies of enoyl reductase. *Science* **1996**, *274*, 2107–2110.

(20) Kitagawa, H.; Kumura, K.; Takahata, S.; Iida, M.; Atsumi, K. 4-Pyridone derivatives as new inhibitors of bacterial enoyl-ACP reductase FabI. *Bioorg. Med. Chem.* **2007**, *15*, 1106–1116.

(21) Seefeld, M. A.; Miller, W. H.; Newlander, K. A.; Burgess, W. J.; DeWolf, W. E., Jr.; Elkins, P. A.; Head, M. S.; Jakas, D. R.; Janson, C. A.; Keller, P. M.; Manley, P. J.; Moore, T. D.; Payne, D. J.; Pearson, S.; Polizzi, B. J.; Qiu, X.; Rittenhouse, S. F.; Uzinskas, I. N.; Wallis, N. G.; Huffman, W. F. Indole naphthyridinones as inhibitors of bacterial enoyl-ACP reductases FabI and FabK. *J. Med. Chem.* **2003**, *46*, 1627–1635.

(22) McMurry, L. M.; Oethinger, M.; Levy, S. B. Triclosan targets lipid synthesis. *Nature* **1998**, *394*, 531–532.

(23) Sivaraman, S.; Sullivan, T. J.; Johnson, F.; Novichenok, P.; Cui, G.; Simmerling, C.; Tonge, P. J. Inhibition of the bacterial enoyl reductase FabI by triclosan: a structure–reactivity analysis of FabI inhibition by triclosan analogues. *J. Med. Chem.* **2004**, *47*, 509–518.

(24) Sullivan, T. J.; Truglio, J. J.; Boyne, M. E.; Novichenok, P.; Zhang, X.; Stratton, C. F.; Li, H. J.; Kaur, T.; Amin, A.; Johnson, F.; Slayden, R. A.; Kisker, C.; Tonge, P. J. High affinity InhA inhibitors with activity against drug-resistant strains of *Mycobacterium tuberculosis*. *ACS Chem. Biol.* **2006**, *1*, 43–53.

(25) Chhibber, M.; Kumar, G.; Parasuraman, P.; Ramya, T. N.; Surolia, N.; Surolia, A. Novel diphenyl ethers: design, docking studies, synthesis and inhibition of enoyl ACP reductase of *Plasmodium falciparum* and *Escherichia coli*. *Bioorg. Med. Chem.* **2006**, *14*, 8086–8098.

(26) Park, H. S.; Yoon, Y. M.; Jung, S. J.; Kim, C. M.; Kim, J. M.; Kwak, J. H. Antistaphylococcal activities of CG400549, a new bacterial enoyl-acyl carrier protein reductase (FabI) inhibitor. *J. Antimicrob. Chemother.* **2007**, *60*, 568–574.

(27) Tipparaju, S. K.; Mulhearn, D. C.; Klein, G. M.; Chen, Y.; Tapadar, S.; Bishop, M. H.; Yang, S.; Chen, J.; Ghassemi, M.; Santarsiero, B. D.; Cook, J. L.; Johlfs, M.; Mesecar, A. D.; Johnson, M. E.; Kozikowski, A. P. Design and synthesis of aryl ether inhibitors of the *Bacillus anthracis* enoyl-ACP reductase. *ChemMedChem* **2008**, *3*, 1250–1268.

(28) Tipparaju, S. K.; Joyasawal, S.; Forrester, S.; Mulhearn, D. C.; Pegan, S.; Johnson, M. E.; Mesecar, A. D.; Kozikowski, A. P. Design and synthesis of 2-pyridones as novel inhibitors of the *Bacillus anthracis* enoyl-ACP reductase. *Bioorg. Med. Chem. Lett.* **2008**, *18*, 3565–3569.

(29) England, K.; am Ende, C.; Lu, H.; Sullivan, T. J.; Marlenee, N. L.; Bowen, R. A.; Knudson, S. E.; Knudson, D. L.; Tonge, P. J.

Slayden, R. A. Substituted diphenyl ethers as a broad-spectrum platform for the development of chemotherapeutics for the treatment of tularaemia. *J. Antimicrob. Chemother.* **2009**, *64*, 1052–1061.

(30) Freundlich, J. S.; Wang, F.; Vilchère, C.; Gulten, G.; Langley, R.; Schiehser, G. A.; Jacobus, D. P.; Jacobs, W. R., Jr.; Sacchettini, J. C. Triclosan derivatives: towards potent inhibitors of drug-sensitive and drug-resistant *Mycobacterium tuberculosis*. *ChemMedChem* **2009**, *4*, 241–248.

(31) Kaplan, N.; Flanner, H.; Hafkin, B. Correlation of AFN-1252 Phase 0 Microdosing and Phase 1 Pharmacokinetics. Presented at the 49th Annual ICAAC Meeting, 2009, San Francisco, CA; F1-2006. Public disclosure from Affinium Pharmaceutical's Web site www.afnm.com.

(32) Ro, S.; Son, K. H.; Kim, Y. E.; Chang, H. J.; Park, S. B.; Choi, J. R.; Cho, J. M. CG400549: Candidate for the Treatment of MRSA Infection. Presented at the 49th Annual ICAAC Meeting, 2009, San Francisco, CA; F1-2007. Public disclosure from CrystalGenomics' Web site www.cgxinc.com.

(33) Schweizer, H. P. Triclosan: a widely used biocide and its link to antibiotics. *FEMS Microbiol. Lett.* **2001**, *7*, 1–7.

(34) Ward, W. H.; Holdgate, G. A.; Rowsell, S.; McLean, E. G.; Pauptit, R. A.; Clayton, E.; Nichols, W. W.; Colls, J. G.; Minshull, C. A.; Jude, D. A.; Mistry, A.; Timms, D.; Camble, R.; Hales, N. J.; Britton, C. J.; Taylor, I. W. Kinetic and structural characteristics of the inhibition of enoyl (acyl carrier protein) reductase by triclosan. *Biochemistry* **1999**, *38*, 12514–12525.

(35) Lyman, F. L.; Furia, T. Toxicology of 2,4,4'-trichloro-2'-hydroxy-diphenyl ether. *IMS, Ind. Med. Surg.* **1969**, *38*, 64–71.

(36) Stewart, M. J.; Parikh, S.; Xiao, G.; Tonge, P. J.; Kisker, C. Structural basis and mechanism of enoyl reductase inhibition by triclosan. *J. Mol. Biol.* **1999**, *290*, 859–865.

(37) Lu, H.; England, K.; am Ende, C.; Truglio, J. J.; Luckner, S.; Reddy, B. G.; Marlenee, N. L.; Knudson, S. E.; Knudson, D. L.; Bowen, R. A.; Kisker, C.; Slayden, R. A.; Tonge, P. J. Slow-onset inhibition of the FabI enoyl reductase from *Francisella tularensis*: residence time and in vivo activity. *ACS Chem. Biol.* **2009**, *4*, 221–231.

(38) Hopkins, A. L.; Groom, C. R.; Alex, A. Ligand efficiency: a useful metric for lead selection. *Drug Discovery Today* **2004**, *9*, 430–431.

(39) Levy, C. W.; Roujeinikova, A.; Sedelnikova, S.; Baker, P. J.; Stuitje, A. R.; Slabas, A. R.; Rice, D. W.; Rafferty, J. B. Molecular basis of triclosan activity. *Nature* **1999**, *398*, 383–384.

(40) Priyadarshi, A.; Kim, E. E.; Hwang, K. Y. Structural insights into *Staphylococcus aureus* enoyl-ACP reductase (FabI), in complex with NADP and triclosan. *Proteins* **2010**, *78*, 480–486.

(41) Irwin, J. J. Community benchmarks for virtual screening. *J. Comput.-Aided Mol. Des.* **2008**, *22*, 193–199.

(42) Hevener, K. E.; Mehboob, S.; Su, P. C.; Truong, K.; Boci, T.; Deng, J.; Ghassemi, M.; Cook, J. L.; Johnson, M. E. Discovery of a novel and potent class of *F. tularensis* enoyl-reductase (FabI) inhibitors by molecular shape and electrostatic matching. *J. Med. Chem.* **2012**, *55*, 268–279.

(43) Payne, D. J.; Warren, P. V.; Holmes, D. J.; Ji, Y.; Lonsdale, J. T. Bacterial fatty-acid biosynthesis: a genomics-driven target for antibacterial drug discovery. *Drug Discovery Today* **2001**, *6*, 537–544.

(44) Kuo, M. R.; Morbidoni, H. R.; Alland, D.; Sneddon, S. F.; Gourlie, B. B.; Staveski, M. M.; Leonard, M.; Gregory, J. S.; Janjigian, A. D.; Yee, C.; Musser, J. M.; Kreiswirth, B.; Iwamoto, H.; Perozzo, R.; Jacobs, W. R.; Sacchettini, J. C.; Fidock, D. A. Targeting tuberculosis and malaria through inhibition of enoyl reductase: compound activity and structural data. *J. Biol. Chem.* **2003**, *278*, 20851–20859.

(45) Rozwarski, D. A.; Vilchère, C.; Sugantino, M.; Bittman, R.; Sacchettini, J. C. Crystal structure of the *Mycobacterium tuberculosis* enoyl-ACP reductase, InhA, in complex with NAD<sup>+</sup> and a C16 fatty acyl substrate. *J. Biol. Chem.* **1999**, *274*, 15582–15589.

(46) Wilson, D. N.; Schluenzen, F.; Harms, J. M.; Starosta, A. L.; Connell, S. R.; Fucini, P. The oxazolidinone antibiotics perturb the ribosomal peptidyl-transferase center and effect tRNA positioning. *Proc. Natl. Acad. Sci. U.S.A.* **2008**, *105*, 13339–13344.

(47) Suller, M. T.; Russell, A. D. Triclosan and antibiotic resistance in *Staphylococcus aureus*. *J. Antimicrob. Chemother.* **2000**, *46*, 11–18.

(48) Villalain, J.; Mateo, C. R.; Aranda, F. J.; Shapiro, S.; Micol, V. Membranotropic effects of the antibacterial agent triclosan. *Arch. Biochem. Biophys.* **2001**, *390*, 128–136.

(49) Denyer, S. P.; Maillard, J. Y. Cellular impermeability and uptake of biocides and antibiotics in Gram-negative bacteria. *J. Appl. Microbiol.* **2002**, *92*, 35S–45S.

(50) Abraham, M. H.; Grellier, P. L.; Prior, D. V.; Duce, P. P.; Morris, J. J.; Taylor, P. J. Hydrogen bonding. Part 7. A scale of solute hydrogen-bond acidity based on log *K* values for complexation in tetrachloromethane. *J. Chem. Soc., Perkin Trans. 2* **1989**, 699–711.

(51) Flo+ is a molecular modeling software developed by Colin McMartin of ThistleSoft; McMartin, C.; Bohacek, R. J. QXP: powerful, rapid computer algorithms for structure-based drug design. *J. Comput.-Aided Mol. Des.* **1997**, *11*, 333.

(52) Bryskier, A.; Soulama, C.; Escaich, S.; Moreau, F.; Vongsouthi, V.; Floquet, S.; Malacain, E.; Walton, A.; Prouvensier, L.; Fischer, S. MUT056399: Mode of Action and Mechanisms of Resistance. Presented at the 50th Meeting of ICAAC, Boston, MA, 2010; Poster F1-832.

(53) Escaich, S.; Prouvensier, L.; Saccomani, M.; Durant, L.; Oxoby, M.; Gerusz, V.; Moreau, F.; Vongsouthi, V.; Maher, K.; Morrissey, L.; Soulama-Mouze, C. The MUT056399 inhibitor of FabI is a new antistaphylococcal compound. *Antimicrob. Agents Chemother.* **2011**, *55*, 4692–4697.

(54) Observed IC<sub>50</sub> > 25 μM in CYP1A2, CYP2C9, CYP2D6, and CYP3A4.

(55) Escaich, S.; Prouvensier, L.; Saccomani, M.; Durant, L.; Malacain, E.; Floquet, S.; Walton, A.; Sam-Sambo, V.; Faivre, F.; Oxoby, M.; Bonvin, Y.; Gerusz, V.; Vongsouthi, V.; Moreau, F.; Soulama, C. MUT056399 Fab I Inhibitor: A New Antibacterial Candidate against *Staphylococcus aureus*. Presented at the 49th Meeting of ICAAC, San Francisco, CA, 2009; Poster F1-2012.

(56) Identified metabolites were the glucuronidated phenol, the sulfated phenol, and the acid resulting from the hydrolysis of the amide. See ref 52 and Sweeney, K.; Henson, C.; McEwen, A.; Read, H.; Wood, S.; Soulama-Mouze, C. [<sup>14</sup>C]-MUT056399: Rat ADME Study with Metabolite Profiling and Identification. Presented at the 51st Meeting of ICAAC, 2011, Chicago, IL; Poster A2-032.

(57) Tsuji, B.; Lanke, S.; Ngo, D.; Soulama-Mouze, C.; Fischer, S.; Forrest, A. Pharmacokinetic–Pharmacodynamic Investigation of MUT056399 against *Staphylococcus aureus* in an in Vitro PD Model. Presented at the 21st Meeting of ECCMID, Milan, Italy, 2011; Poster P783.

(58) Soulama-Mouze, C.; Bryskier, A.; Chassard, D.; Fischer, S. MUT056399: A Single Intravenous Ascending Dose Study in Healthy Human Volunteers. Presented at the 21st Meeting of ECCMID, Milan, Italy, 2011; Poster P1510.

(59) Compound **83**, referred in the literature as MUT056399, is currently undergoing clinical development by FAB Pharma.